

# **Mechanistic Model and Optimization of the Diclofenac Degradation Kinetic for Ozonation Processes Intensification**

**Bryan Acosta-Angulo<sup>1</sup>, Jose Lara-Ramos<sup>2</sup>, Jennyfer Diaz-Angulo<sup>3</sup>, Miguel Angel Mueses<sup>1</sup> and Fiderman Machuca-Martínez<sup>2,\*</sup>**

<sup>1</sup> Modeling & Application of Advanced Oxidation Processes, Photocatalysis & Solar Photoreactors Engineering, Chemical Engineering Program, Universidad de Cartagena, 1382-Postal 195, Cartagena, Colombia; bacostaa@unicartagena.edu.co (B.A.-A.); mmueses@unicartagena.edu.co (M.A.M.)

<sup>2</sup> GAOX, CENM, Escuela de Ingeniería Química, Universidad del Valle, 760032, Cali, Colombia; lara.jose@correounivalle.edu.co

<sup>3</sup> Research Group in Development of Materials and Products GIDENMP, CDT, ASTIN SENA, Tecnoparque 76003, Colombia; jdiazan@sena.edu.co

\* Correspondence: fiderman.machuca@correounivalle.edu.co; Tel.: +57-31-6448-7088

## **Content**

Table S1. Parameters of the Six-Flux Model. Table S2. Computed mass transfer constants. Figure S1. Diclofenac concentration based on a first order rate law for the ozonation process. Figure S2. Diclofenac concentration based on a first order rate law for the catalytic ozonation process. Figure S3. Diclofenac concentration based on a first order rate law for the photocatalytic ozonation process. Table S3. Electrical energy per order for each process conditions.

### S1. Six-Flux Model parameters

In Table S1 were presented the constants required to compute the LVRPA for a given point at the flotation cell based in equations (x-y). The scattering and absorption coefficients were taken for the Evonik p25.

Table S1. Constants employed to estimate the LVRPA.

| Constants              |          | Value                 | Units                           |
|------------------------|----------|-----------------------|---------------------------------|
| Intensity              | $I_0$    | $2.06 \times 10^{-5}$ | <i>Einstein</i> $s^{-1} m^{-2}$ |
| Scattering coefficient | $\sigma$ | 5420                  | $m^2 kg^{-1}$                   |
| Absorption coefficient | $\kappa$ | 287                   | $m^2 kg^{-1}$                   |

First, the scattering albedo  $\omega_{corr}$  was computed according to Equation (S1), then, by replacing within Equations (S2) and (S3), the corrected value for this variable was obtained (S4). Here  $p_s$ ,  $p_b$ , and  $p_f$  were the sides, backward and forward scattering probabilities.

$$\omega = \frac{\sigma}{\kappa + \sigma} \quad (S1)$$

$$a = 1 - \omega p_f - \frac{4\omega^2 p_s^2}{1 - \omega p_f - \omega p_b - 2\omega p_s} \quad (S2)$$

$$b = \omega p_b + \frac{4\omega^2 p_s^2}{1 - \omega p_f - \omega p_b - 2\omega p_s} \quad (S3)$$

$$\omega_{corr} = \frac{b}{a} \quad (S4)$$

This value was used to calculate the corrected wavelength  $\lambda_{corr}$  and the optical thickness  $\tau$  according to Equations (S5) and (S6). Then, the apparent value for the optical thickness  $\tau_{app}$  was computed from (S7). Finally, the six-flux model parameter  $\gamma$  was obtained by equation (S8).

$$\lambda_{corr} = \frac{1}{a(\sigma + \kappa)C_{mp}\sqrt{1 - \omega_{corr}^2}} \quad (S5)$$

$$\tau = (\sigma + \kappa)C_{mp}r_p \quad (S6)$$

$$\tau_{app} = a\tau\sqrt{1 - \omega_{corr}^2} \quad (S7)$$

$$\gamma = \frac{1 - \sqrt{1 - \omega_{corr}^2}}{1 + \sqrt{1 - \omega_{corr}^2}} \exp(-2\tau_{app}) \quad (S8)$$

### S2. Mass Transfer

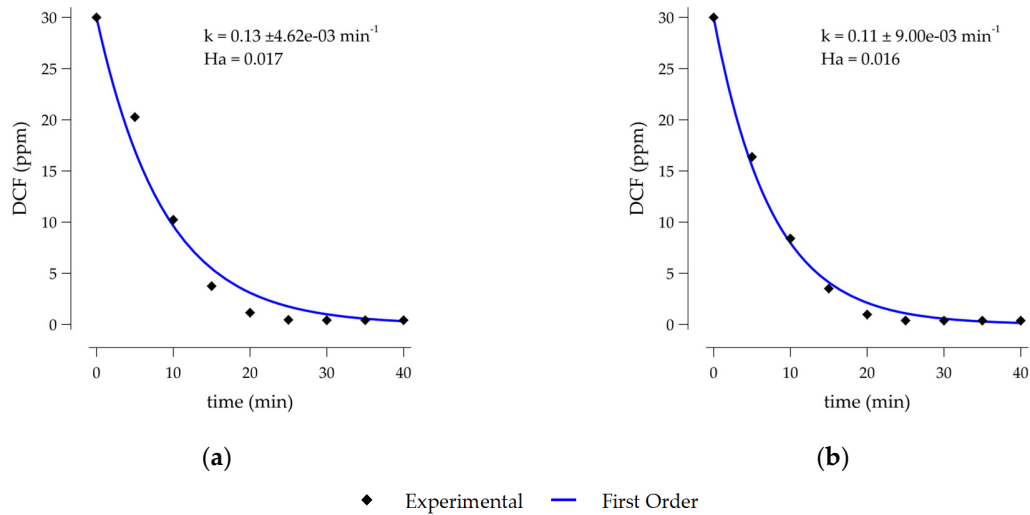
The estimated values for the mass constants at the flotation cell were summarized in Table S2.

Table S2. Mass transfer constants for the flotation cell.

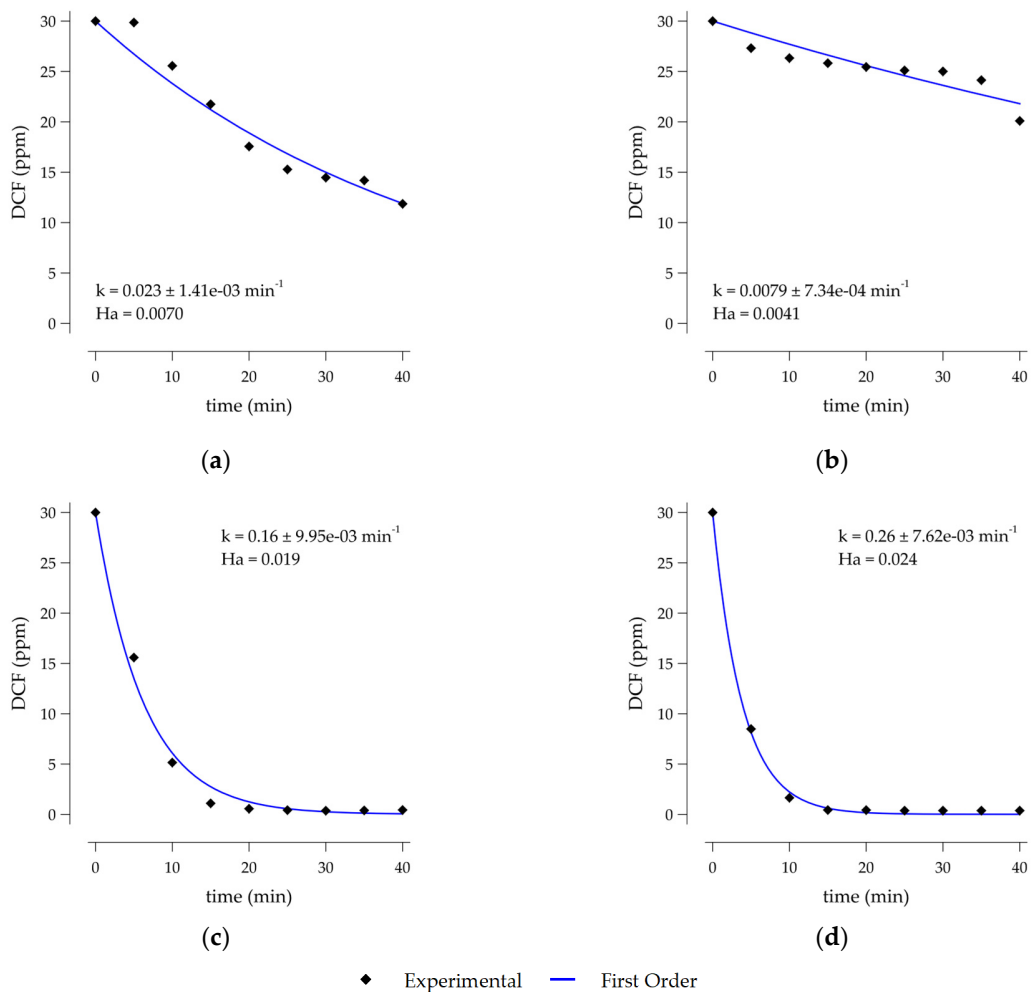
| Constants    | Value                 | Units                  |
|--------------|-----------------------|------------------------|
| $k_L$        | $4.56 \times 10^{-3}$ | $m \text{ min}^{-1}$   |
| $a$          | 220.33                | $m^{-1}$               |
| $\phi_{(g)}$ | $4.13 \times 10^{-3}$ | ---                    |
| $d_b$        | 0.11                  | $mm$                   |
| $D_{O_3}$    | $7.80 \times 10^{-8}$ | $m^2 \text{ min}^{-1}$ |

### S3. Kinetic Regime

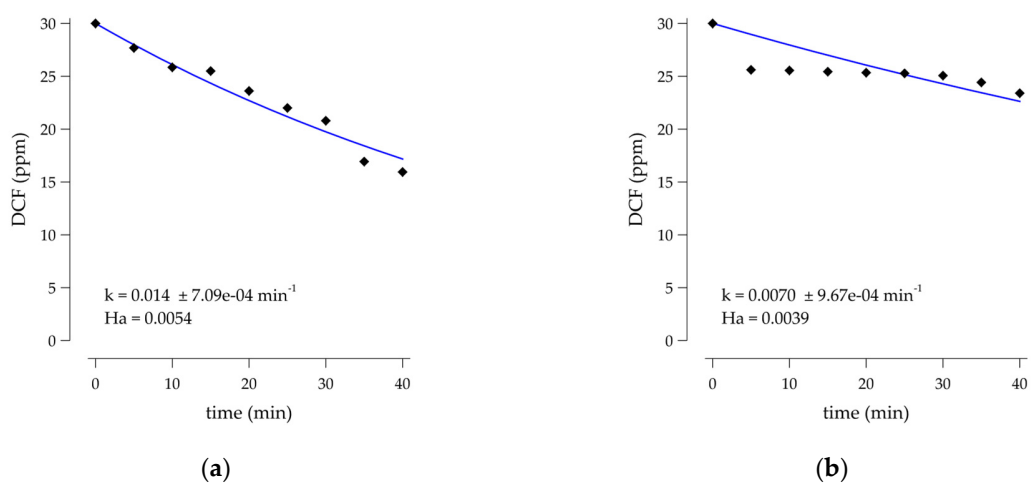
Figures S1–S3 depicted the estimated values of the Hatta number based on a first-order rate law for the ozonation, catalytic ozonation, and photocatalytic ozonation processes.



**Figure S1.** First-order rate law predictions for the diclofenac concentration in the ozonation process at (a) 2.66 and (b) 7.44 ppm in the ozone dose.



**Figure S2.** First-order rate law predictions for the diclofenac concentration in the catalytic ozonation process at (a) 2.66 & 300, (b) 2.66 & 800, (c) 7.40 & 300, (d) 7.40 & 800 ppm in the ozone dose and the catalyst load respectively.



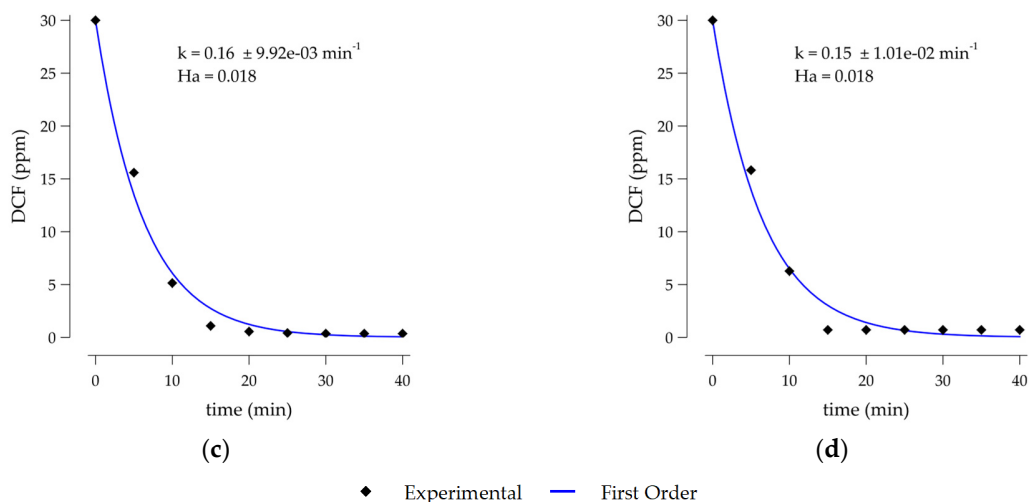


**Figure S3.** First-order rate law predictions for the diclofenac concentration in the photocatalytic ozonation process at (a) 2.66 & 300, (b) 2.66 & 800, (c) 7.40 & 300, (d) 7.40 & 800 ppm in the ozone dose and the catalyst load respectively.

#### S4. Electrical Energy per Order

**Table S3.** Electrical energy per order (EE/O) for each process conditions.

| Process                  | Ozone dose (ppm) | Catalyst load (ppm) | EE/O ( $kWh\ m^{-3}$ ) |
|--------------------------|------------------|---------------------|------------------------|
| Ozonation                | 2.66             | ---                 | 14.44                  |
|                          | 7.40             | ---                 | 17.07                  |
| Catalytic Ozonation      | 2.66             | 300                 | 81.62                  |
|                          | 2.66             | 800                 | 237.64                 |
|                          | 7.40             | 300                 | 11.73                  |
|                          | 7.40             | 800                 | 7.22                   |
| Photocatalytic Ozonation | 2.66             | 300                 | 158.47                 |
|                          | 2.66             | 800                 | 316.45                 |
|                          | 7.40             | 300                 | 13.86                  |
|                          | 7.40             | 800                 | 14.79                  |